

HIGH STRENGTH, TOUGHNESS AND NANOSTRUCTURE CONSIDERATIONS FOR FE/CR/MN/C LATH MARTENSITIC STEELS

Dr. Greg Kusinski - MMFX Technologies Corporation, 2415 Campus Drive Suite 100,
Irvine, CA 92612, USA, greg.kusinski@mmfx.com

Prof. Gareth Thomas – MMFX Technologies and Department of Materials Science,
University of California, Berkeley, USA, garth@berkeley.edu

ABSTRACT

Examples are given of multilayer design of martensitic steels from the microstructural viewpoint. The design criteria for steels with superior strength-toughness-corrosion properties based on a multilayered microstructure composed of dislocated lath martensite and retained austenite are presented. The paper discusses the above principles in relation to the design of superior steels based on the series of Fe/Cr/Mn/C steels (designated HS-MMFX, Fig. 4 and MMFX for example Table 2), which satisfy these design criteria, so as to achieve the described microcomposite structure as revealed by advanced electron microscopy analyses, such that for very high strength applications adequate toughness must also be attained for safe applications. Some further examples for corrosion resistance are also made. Another main advantages of these high strength steels is the 30 – 50% weight savings that become available and thus impact strongly on transportation and construction developments.

KEYWORDS

Microstructure, lath martensite, retained austenite, corrosion resistance, TEM

INTRODUCTION

The conventional methods for increasing the strength of alloys are based on reducing dislocation mobility by alloying, e.g. in solution (carbon in steel is a prime example), dispersed particles, dislocation multiplication, and so on. Such methods by definition greatly reduce plastic flow and, hence, reduce toughness. It is now quite well recognized that to optimize and design materials for specified properties, materials are best utilized as composites. The development of high-strength steels requires multicomponent microstructures designed and processed at the micron and nanometer levels. In particular, the multilayered arrangement of strong (dislocated martensite) and ductile (austenite or ferrite) phases in steels is attractive for mechanical and many functional properties (e.g. toughness and corrosion resistance). In the case of certain carbon steels such composite structures (martensitic laths with thin films of retained austenite) can be obtained if the composition and processing are well controlled [1-3]. Likewise, one must avoid unwanted composites (ferrite – upper bainite with grain boundary carbides, and temper embrittled martensites are examples). Martensites are complex, and in our earlier work we have shown the relationship between dislocated martensite (steels with the

martensite start temperature (T_{MS}) above about 300°C) and twinned martensite (steels with T_{MS} below 300°C) and their strength and toughness properties and methods for optimizing these properties [1, 3-7]. Clearly, the M_s temperature determined by the total alloy content is a useful design parameter. As reported in our earlier references, twinned martensitic steels containing carbon are brittle and will not be discussed here (as opposed to certain FeNi alloys) [8, 9]. Nevertheless, there is a limit to wt% C so as to avoid twinning and, hence, a limit to strength. Thus the emphasis here is on dislocated lath martensite. In order to understand the properties of any such multilayered system, and hence to be able to design pre-determined sets of properties, it is necessary to know their structure. For this reason, characterization of micro and nano-structures at relevant length scales is of particular importance [10-12]. Electron microscopy is thus a requirement in order to establish structure-property relations.

A. STRUCTURE AND MECHANICAL BEHAVIOR

1. MICROSTRUCTURE

Typical microstructures obtained by cooling austenite at rates that transform it to pearlite (slow) to bainite to martensite (fast) are shown schematically in Fig. 1. Thus, in order to obtain dislocated lath martensite, fast cooling (depending on composition) will be required. Packet lath martensite is a desirable transformation for optimization of mechanical properties, and for this reason chemical composition and processing are designed and tightly controlled.

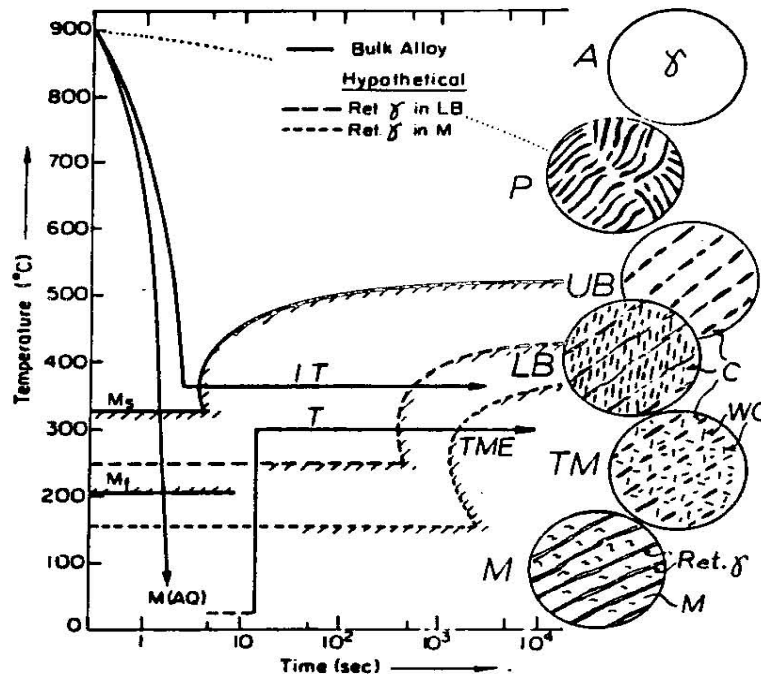


Fig. 1. Schematic diagram showing microstructures obtained by cooling austenite, after M. Sarikaya.

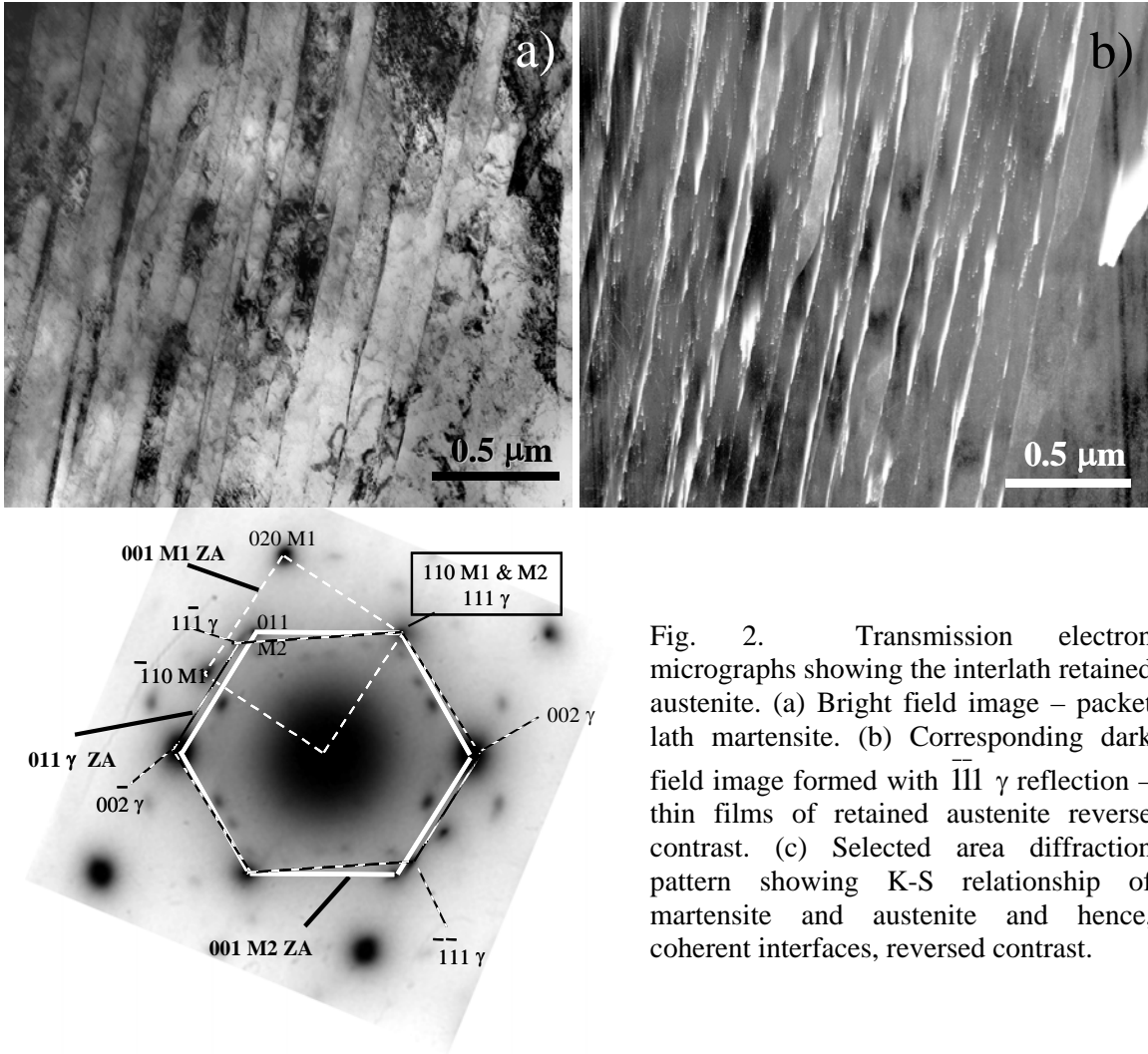


Fig. 2. Transmission electron micrographs showing the interlath retained austenite. (a) Bright field image – packet lath martensite. (b) Corresponding dark field image formed with $\bar{1}\bar{1}1$ γ reflection – thin films of retained austenite reverse contrast. (c) Selected area diffraction pattern showing K-S relationship of martensite and austenite and hence, coherent interfaces, reversed contrast.

Fig. 2 shows an actual example of the multilayered austenite/martensite microcomposite (note the scale of the multilayer structure in the packet). The multilayer composite contains the tough work-hardened laths of martensite linked coherently (with the Kurdjumov-Sachs K/S orientation relation) to the untransformed, ductile austenite, giving a packet of alternating layers of austenite (~50 atoms wide) and dislocated martensite laths. Unlike conventional pearlitic/bainitic microstructures, there are no carbides (and ideally no inclusions), and the high strength, high toughness derives from this microstructure. The key to attractive properties is in maintaining the multilayer austenite-martensite composites in the packets by keeping the martensite start temperature (T_{MS}) above ~320°C and cooling fast enough to avoid non-martensitic products. Such microstructures offer a range of attractive properties, including weight saving, and some examples are summarized below.

It is now well known that the strength of lath martensitic steels is controlled primarily by the wt. %C in solution, and the dislocation density, Fig. 2. Dislocated martensite has a high dislocation density and is thus work hardened. The carbon-dislocation interactions provide linear hardening, provided the martensite is dislocated, and this sets the

maximum wt.% C at about 0.4, depending on the total alloy content for example Cr. For certain properties it is also beneficial to precipitate nano-sized carbides and carbo-nitrides within martensitic laths. On the other hand, precipitates at grain boundaries and lath boundaries must be avoided to optimize toughness and corrosion resistance. In dual (martensite and ferrite) [13] or triple phase steels (martensite, ferrite and retained austenite) [14, 15], the strength is mainly derived from the volume fractions of the phases present, notably martensite and ferrite as in $\sigma_C \sim \sigma_\alpha f_\alpha + \sigma_M f_M$, (C = Composite, α = Ferrite, M = Martensite), of which the most important term is $\sigma_M f_M$ [16]. In the case of triple phase steels, the strong martensite phase is actually a nano-composite mixture of dislocated laths and interlath retained austenite. The retained austenite, which is stabilized mainly by carbon during the final rolling-cooling, also contributes to improved ductility (cold forming), and toughness.

Table 1. Carbides formed as a result of $\gamma \rightarrow \alpha + C$ decomposition [17].

Feature	Martensite	Bainite Lower	Bainite Upper
Laths in Packets	High dislocation density	Dislocated ferritic laths	Low dislocation density ferritic laths
Common Direction	Lath faces $\langle 110 \rangle_M$	Lath faces $\langle 110 \rangle_B$	Irregular
Interlath Region	Quenched - Continuous retained austenite; Tempered - stringers of M_3C (TME)	Non-continuous retained austenite (short isothermal) or carbides (long isothermal)	Mostly carbides as in tempered martensite, TME
A/F Interface Austenite Stability Interface plane	Enriched can be very stable (110)M// (111)A	Some C enrichment not very stable (110)B// (111)A	N/A
A/F orientation relationships	K-S to G-T to N-W	K-S to G-T to N-W	N/A
Twin Relation of Laths	(110) M plane	(112)F plane	Not observed
A/F microscopic habit	(111)A	(111)A	Inferred
Carbides and Orientation	Widmanstätten	Unidirectional	At boundaries
Relationship	Bagaryatskii (110)M// (100)C (111)M// (010)C (112)M// (001)C	Isaichev (111)B// (010)C (011)B// (103)C	
Mechanism of Transformation	Shear + interface C diffusion and autotempered carbide precipitation	Shear + C diffusion interlath carbide precipitation	Low dislocation density ferrite, some shear + C diffusion interlath carbides

A = Austenite, B = Bainite, M = Martensite

The morphology of carbides in such steels (Fig. 1) varies continuously from grain boundary laths (upper bainite) to small globular particles as in lower bainite. An important question is where and when the carbides formed as a result of $\gamma \rightarrow \alpha + C$ decomposition. These carbides will have crystallographic characteristics depending on where and on which phase the carbides nucleate and grow. A partial summary of these relations is shown in Table 1. Due to the fine scale of many such microstructures, determining the details of microstructure evolution require the application of precise electron microscopy and microdiffraction.

2. MECHANICAL PROPERTIES

Steels used commercially must also satisfy other requirements, such as fracture and corrosion resistance [18, 19]. The avoidance of micro galvanic cells in the microstructure, typically at ferrite or martensite/austenite boundaries, can considerably improve corrosion resistance. It is here that the microcomposite martensite/austenite and the dual/triple phase steels offer attractive combinations of high strength, corrosion resistance and toughness.

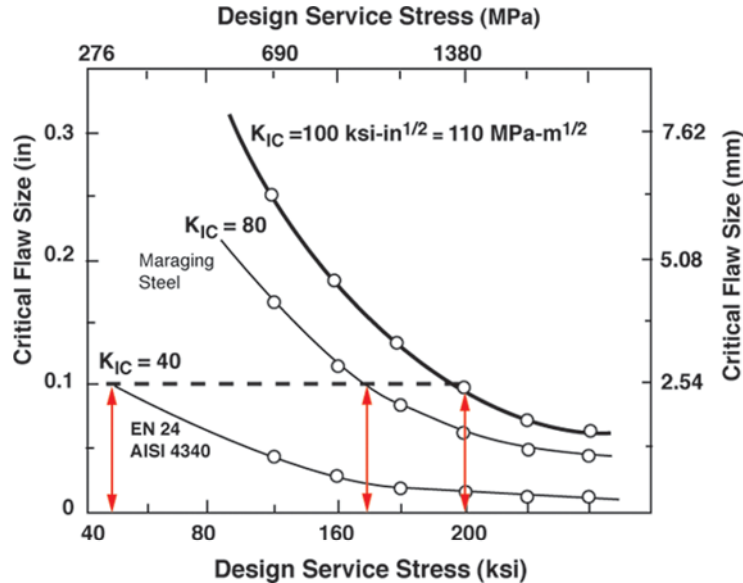


Fig. 3. Plot of critical flaw size versus design stress for steels of similar yield strength.

Toughness can be synthesized in two broad categories, a) fracture initiation, as indicated by the Charpy test, and b) propagation of cracks, as indicated by the K_{IC} type testing, also in different environments. Generally the Charpy toughness is greater the smaller the grain size, or in the case of lath martensites--the packet size, which depends on the prior austenite grain size. This is an important measure of the toughness-temperature relations to ascertain the performance of steels at low temperatures--again high strength, high toughness to -100°C is needed to avoid the ductile to brittle transition is service for many applications. Fig. 3 shows the relation between critical crack size, K_{IC} , and applied stress as derived under plane strain conditions. This figure shows that designing for high strength is only practical if also the K_{IC} properties are designed to take advantage of the strength. As an example a steel A with 3 times the strength of steel B, but with 1/3 of its K_{IC} , is only safe at stresses below the design strength of A.

The compromise between strength and toughness, can be mitigated with the use of composites-mixtures of tough, ductile and strong phases, paying attention to composition and morphology. Fig. 4 and Fig. 7 are examples of the range of properties attainable from the simple Fe/0.3C/4Cr composites (with quaternary Mn alloying).

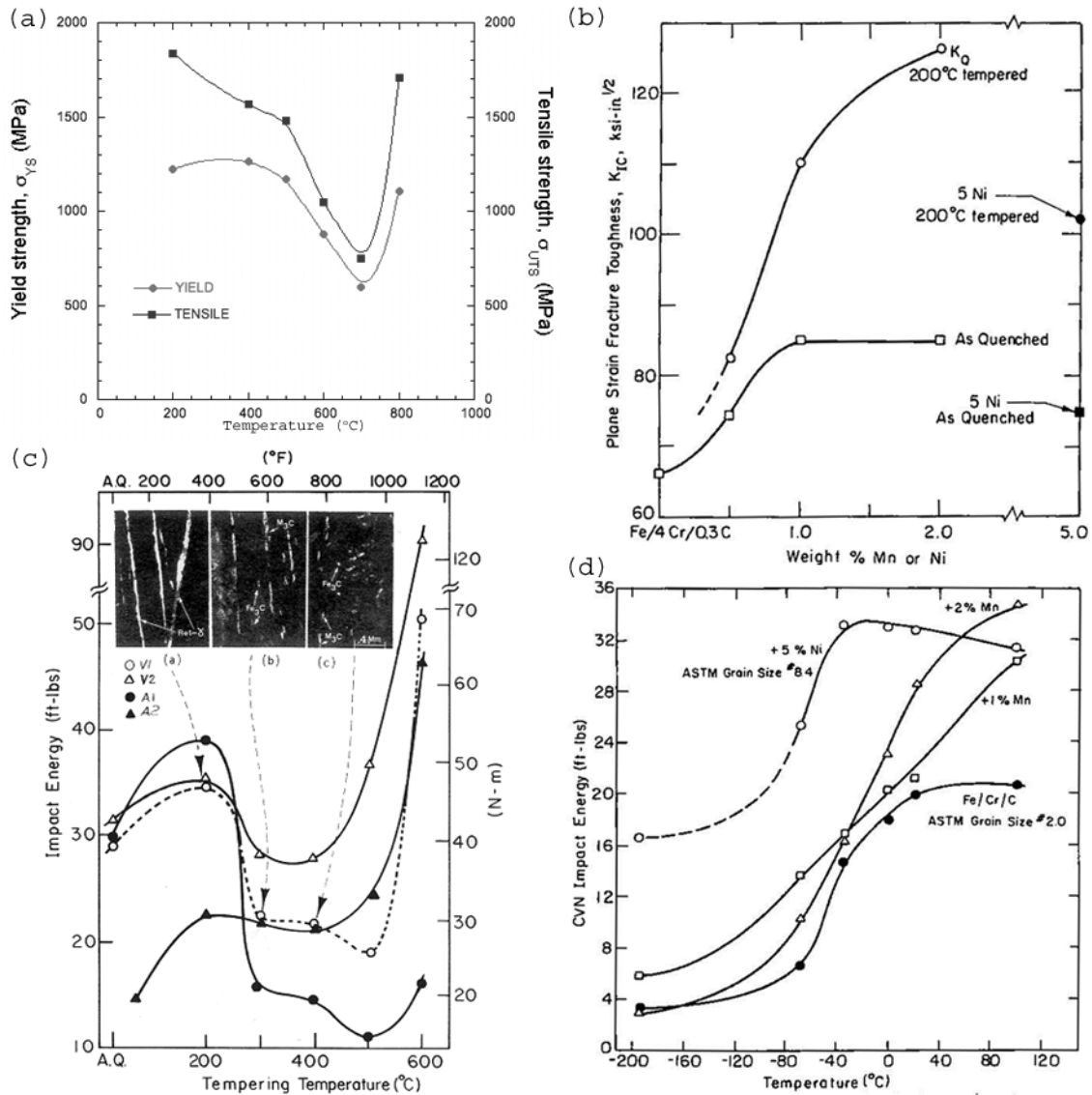


Fig. 4. Alloys HS-MMFX with the base chemical compositions Fe/0.3C/4Cr. (a) Yield and Tensile strength vs. tempering temperature. (b) K_{IC} vs. quaternary alloying [3], (c) Charpy V-notch energy revealing both TME and TE regions [17], (d) Ductile-brittle transition curves vs. quaternary alloying [3].

3. MORPHOLOGICAL FACTORS

Whilst great attention is paid to the identification and fraction of phases present in alloys, it is also realized that morphology plays an important role in property management and as such must be brought into the alloy design scheme. One example we choose to illustrate this point is that of the quenched/tempered/isothermal ageing conditions in strong steels. In the as quenched condition (dislocated multilayered martensite sandwiched with untransformed austenite) Fig. 5a-1, slip can easily cross from lath to lath via the austenite because $\{110\}_\alpha$ parallels $\{111\}_\gamma$ and $\{110\}$ are the likely slip planes in martensite. Upon

plastic deformation, due to the coherent fcc/bcc crystallography, slip can easily pass from the martensite across to austenite and into the next lath, see schematic in Fig. 5a-1. The result is a large plastic zone and good crack blunting by slip (Fig. 5a-1) leading to high fracture toughness (K_{IC}). Since the strength depends almost entirely on the %C in martensite, it is easy to control strength and toughness by maintaining this microstructure up to the limits required by the design engineers.

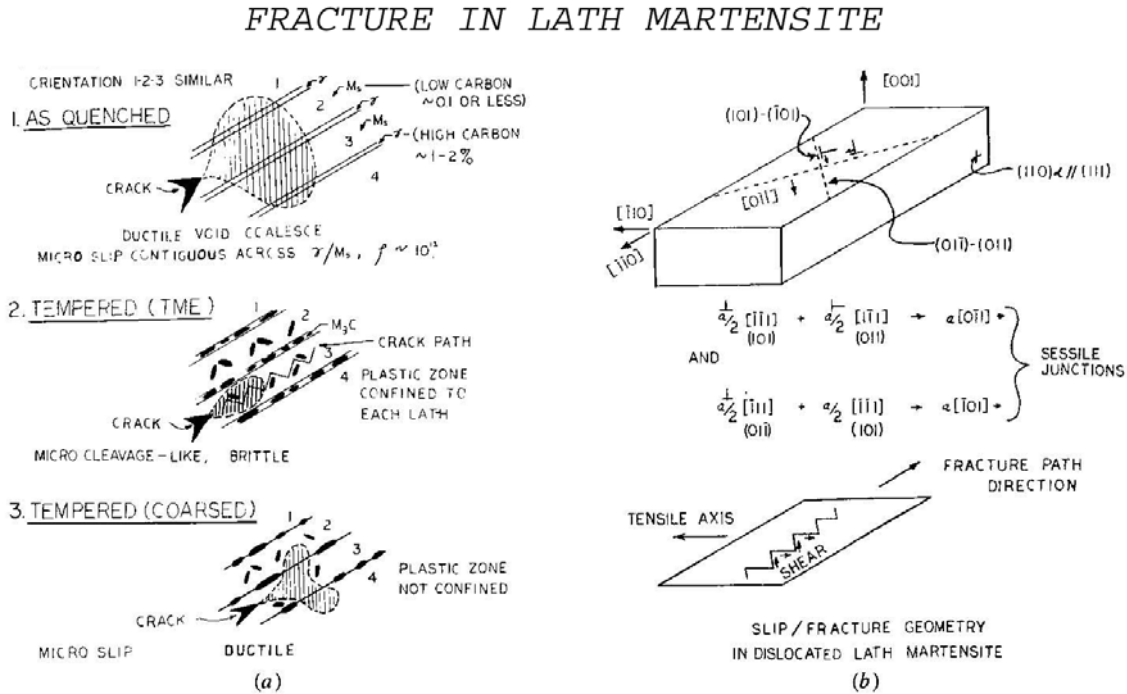


Fig. 5. (a) Schematic line drawing showing the influence of microstructure on plastic zone and fracture path. (b) Slip within a martensite lath could lead to immobile $[01\bar{1}]$ type dislocations. Slip also occurs on the $\{110\}$ planes containing intralath Fe_3C after tempering, giving rise to local zig-zag fracture [17].

Taking the case of tempering lath martensites, when tempering is done so as to limit precipitation to small Widmanstätten intralath carbides, no degradation in mechanical properties is observed. However, when the austenite decomposes into films of cementite, as shown in Fig. 5a-2, slip is very restricted in its ability to cross from lath to lath, confining the plastic zone to a single lath, giving a small critical crack size and poor toughness i.e. low K_{IC} values. This microstructure is known to be a major factor in the low toughness known as Temper Martensite Embrittlement (TME) in Quench & Temper treatments ($300^\circ C - 500^\circ C$), and also in “classical” upper bainite, which is schematically the same as that of Fig. 5a-2, thus these microstructures are morphologically the same. As is also well known tempering beyond the stages of Fig. 5a-2 tends to spheroidise the particles (Fig. 5a-3), opening up the slip path across laths again. The similarity to “classical” LOWER BAINITE is clear [17].

4. RETAINED AUSTENITE

It is clear that the retention of austenite in appropriate morphologies e.g. nano layers between the dislocated martensite laths provides attractive features, e.g. the (1) TRIP phenomena (Transformation Induced Plasticity): In many carbon steels the retained austenite has been shown to be present at about 6% and is partially stabilized mainly through carbon redistribution within austenite and at austenite/martensite boundaries. Current practice to allow such carbon redistribution usually involves interrupted cooling from the final rolling at about 500°C. However, the microstructure of the nano multilayered lath martensite/retained austenite (α'/γ) steels does not require such interrupted cooling. The characterization of the carbon distribution is difficult to do by spectroscopy analysis but methods such as atom probe [17, 20] and electron micro diffraction [21] have confirmed that the carbon concentration in austenite may rise to 2 wt.% and vary in value – including >5 at % at the γ/α' interface. Thus there is stabilization by carbon (lowering T_{MS} to low values), and morphology. The austenite can, however, be partially stable and may be prone to decomposition to iron and alloy carbides. The effect is detrimental to toughness especially at interlath boundaries and leads to the above mentioned Temper Martensite Embrittlement (TME), which is not to be confused with Temper Embrittlement (TE), which is caused by impurity segregation at prior austenite grain boundaries during processing: i.e. fracture by TME is intergranular in martensite, whereas, fracture by TE is at the prior austenite boundaries.

Mechanical stability; the metastable austenite can also contribute to the TRIP phenomenon, which allows TRIP steel to be cold formed with high ductility but also work hardens during forming due to stress induced transformation of austenite leading to a strong product. The disadvantage is the thermal arrest, which is employed during final rolling so as to allow carbon to redistribute into austenite and stabilize it for the cold forming sequence.

B. CORROSION IN CONCRETE

1. CORROSION PROBLEMS

One of the major problems facing the construction industry today is the effect of corrosion of steel reinforcement. For example, in the United States alone, approximately 50,000 concrete reinforced bridges are considered structurally deficient due to corrosion of steel reinforcement. It is estimated that the annual direct cost to repair such deficient bridges is between \$7 billion to \$10 billion [22]. The aggressive nature of deicing salts (via introduction of Cl^- ions) is well documented and it is reported that the salt use has in fact increased in the last decade. The need for corrosion-resistant steel is motivated by the billions of dollars required annually to reconstruct or repair structures whose design life has been either shortened or eliminated as a result of corrosion.

The design of the Fe/Cr/Mn/C steels described above included considerations of corrosion-resistance. Prior to this, the corrosion of steel rebar was treated either by coatings (i.e. paints, epoxies, galvanization, or metal plating), substitution with expensive alloyed steels (i.e. stainless steel), use of greater concrete covers or addition of

admixtures to improve the quality of concrete. Epoxy-coated rebar has been used for approximately 25 years but its limitations are becoming of great concern and its use is declining [23-25]. Another rebar protective measure is to provide a greater concrete cover over the steel reinforcement. This thicker layer of concrete slows salt penetration and improves service life. Unfortunately, as more concrete is added, more steel must also be added. Consequently, the whole structure becomes larger, heavier, and more expensive to construct. Stainless-steel rebar is far superior to conventional rebar, and may provide 100+ years economic service life. However, high cost makes stainless steel a cost-prohibitive material for most construction applications.

2. NEW STEELS FOR CORROSION RESISTANCE IMPROVEMENT

The Microcomposite steel rebars [19, 26], based on the microstructures described above, also correct the steel corrosion problem by the elimination of micro galvanic cells in the steel structure, thus minimizing corrosion initiation. Typical alloy compositions are shown in Table 2. In these MMFX steels Cr is an important alloying element since it is known that Cr drastically reduces the corrosion rate. The effect of the chromium content on the corrosion resistance of the steel is illustrated in Fig. 6 [27], which shows that the chromium content of (9 wt.% to 10 wt.%) can provide corrosion resistance characteristics similar to some stainless steels when tested under similar environmental conditions. Independent tests conducted by the Virginia Transportation Research Council [28] showed that the Critical Chloride Threshold Level (CCTL) for MMFX2 reinforcement is 5 to 6 times greater than that for conventional A615 rebar and 1.75 greater than that for 2101 solid stainless steel bars.

Table 2. Typical chemical composition (weight %) of MMFX2 reinforcing bar.

Element	C	Cr	Mn	N	P	Si
wt.%	0.10	8 to 11	1.5	0.04	0.02	0.50

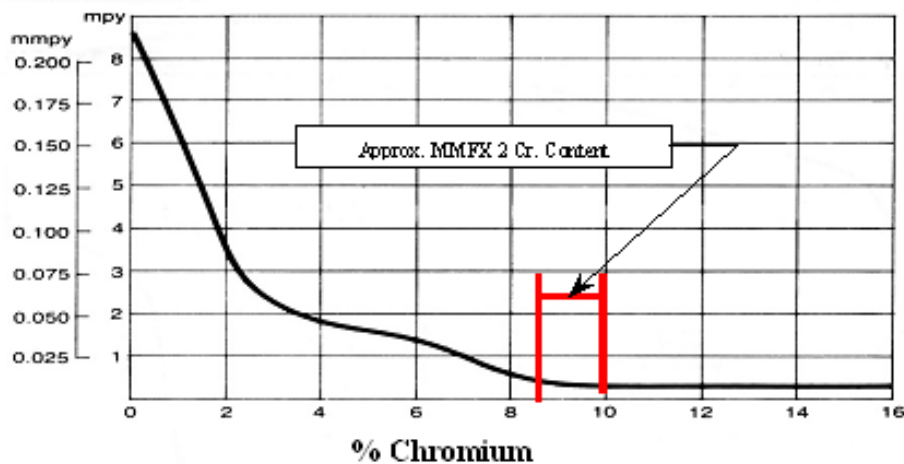


Fig. 6. Effect of chromium content on corrosion rate [27].

3. PROPERTY COMPARISON

Fig. 7 compares some properties of the multilayered steels with commercial ASTM A615 steel (ferrite – pearlite). As shown in Fig. 7(a), the MMFX2 steel rebar tensile properties conform to the following ASTM A1035 standard:

Minimum Tensile Strength: 150,000 psi, 1035 MPa
 Minimum Yield Strength: 100,000 psi, 690 MPa
 Minimum Ultimate Elongations: 7%

The stress-strain curve of the MMFX2 steel rebar reflects a continuous work hardening behavior, without a well-defined yield point. It can be modeled utilizing the following relationship of stress and strain: $f_s = 165 (1 - e^{-185\varepsilon})$. Due to the lack of a well-defined yield plateau, the yield strength for structural engineering calculations, is taken as the stress corresponding to a particular strain.

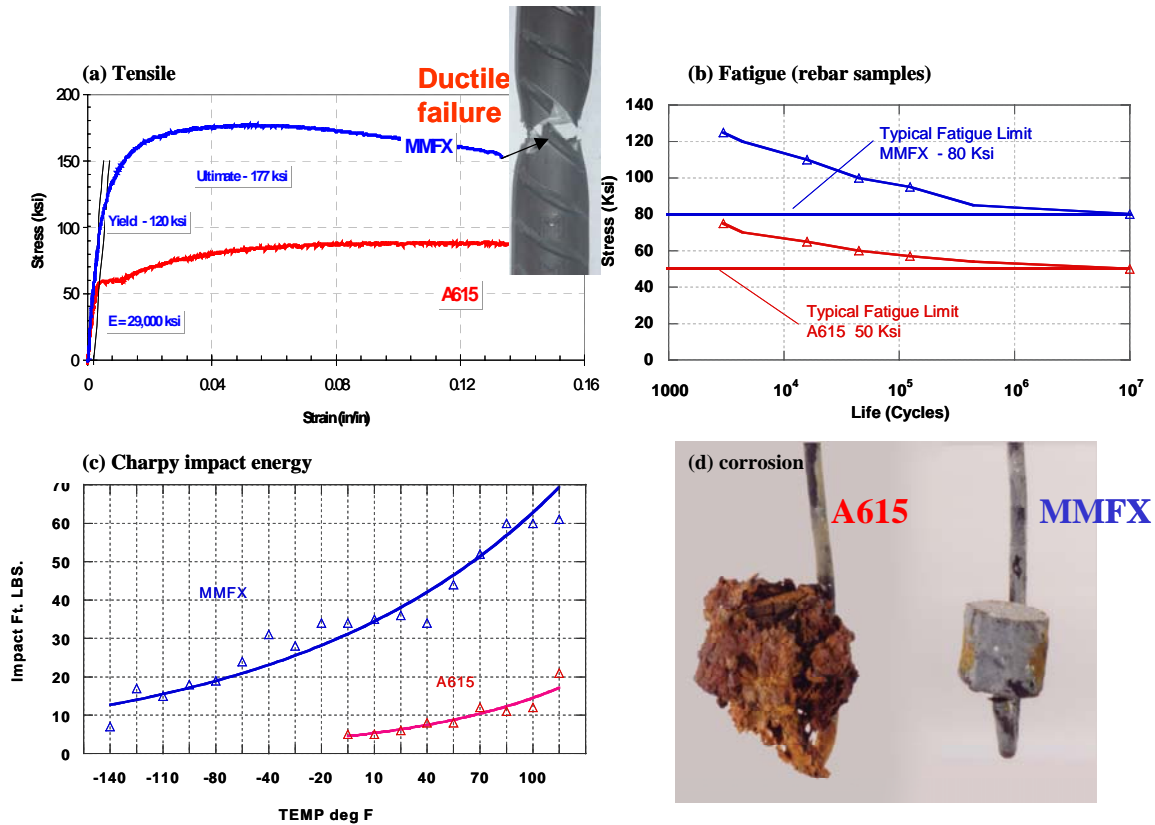


Fig. 7. (a) The tensile properties of MMFX2 steel compared to ASTM A615 ferrite-pearlite steel, (b) the superior fatigue properties compared to A615, (c) superior low temperature Charpy toughness, (d) corrosion samples after several weeks in 3% chloride. Note the A615 steel is almost totally destroyed by corrosion.

4. CONCRETE DESIGN WITH HIGH STRENGTH STEEL BARS

The design of concrete members reinforced with high-strength rebars for flexure is analogous to the design of concrete reinforced with conventional steel bars. Experimental data on concrete members reinforced with bars show that flexural capacity can be calculated based on similar assumptions for members reinforced with A615 carbon steel rebars, taking into account the higher strength of the bars.

Based on such guidelines, several categories of application would seem to be beneficial. One example is high strength concrete structures. In addition to the high corrosion resistance, the high-strength properties of MMFX2 rebars can be best utilized in combination with high-strength concrete in application requiring concrete strengths over 8,000 psi. In areas of seismic zones, the high strength property of the MMFX2 rebar is ideal for applications where confinement of compressive elements as spirals, stirrups, joint steels and columns ties becomes very beneficial avoiding congestion of reinforcement.

Because all projects are driven by economics, the proper utilization of high strength, tough steels requires that the designers consider effects that a higher strength material has on the overall design of the structure, along with its durability. First, the size of the member needs to be studied to insure that the higher strength MMFX reinforcement is being fully utilized. Next, the corrosion resistance of the reinforcement allows the designer to reduce many costly concrete additives that would otherwise be required.

Although the MMFX2 rebar has a premium cost on a per pound basis over conventional steel, it has been found that when designed utilizing the materials strength substantial up front cost savings can be realized. For example, the analysis done on a 490 foot high rise building in Las Vegas, Nevada, that was originally designed using conventional A615-Gr60(420 MPa) steel and subsequently redesigned utilizing MMFX2 Gr100 (690 MPa) rebar, showed an overall 40% reduction in the amount of steel used. This reduced the cost of the installed material by 16%, and at the same time greatly simplifying the placement of steel in highly congested areas.

SUMMARY

We have shown the principles of steel alloy design using Fe/C/Cr/Mn alloys to produce nanophase multilayered structures of dislocated martensite or ferrite separated by sheets of untransformed austenite and free from interlath carbides, for optimal strength and corrosion resistance. An example is given for steel reinforcing material. The approval of ASTM A1035-Gr 100 ksi (690MPa) steel, allows the replacement of weaker (e.g. ASTM A615-grade 60 ksi (420 MPa) steels by these high strength bars. Structural engineering calculations show that in certain cases it is possible to achieve up 50-60% steel reduction. Furthermore, these principles could also be applied for transportation and other applications.

REFERENCES

- 1) G. THOMAS, Metallurgical Transactions A 9A, (1978), p.439.
- 2) G. THOMAS, ISI International 46, (1973), p.451.
- 3) B.V.N. RAO and G. THOMAS, Metallurgical Transactions A 11A, (1980), p.441.
- 4) B.V. NARASIMHA RAO and G. THOMAS, Materials Science and Engineering 20, (1975), p.195.
- 5) M.F. CARLSON, B.V.N. RAO and G. THOMAS, Metallurgical Transactions A Vol. 10A, (1979), p.1273.
- 6) G. KRAUSS and A.R. MARDER, Metallurgical Transactions A 2, (1971), p.2243.
- 7) B.V.N. RAO and G. THOMAS, Materials Science and Engineering 20, (1975), p.195.
- 8) G. THOMAS and G. KUSINSKI, Proc.19th ASM Heat Treating Conference" p. 515.
- 9) G.J. KUSINSKI and G. THOMAS, in "Nano and Microstructural Design of Advanced Materials", edited by M.A. Meyers, R.O. Ritchie and M. Sarikaya (Elsevier, 2003) p. 81.
- 10) M. SARIKAYA, K. EASTERLING and G. THOMAS, Electr. Micr. 1, (1980), p.176.
- 11) G. THOMAS, Metallurgical Transactions A 2, (1971), p.2373.
- 12) G. THOMAS, Acta Microscopica 1, (1992), p.1.
- 13) J.Y. KOO and G. THOMAS, Metallurgical Transactions A 8A, (1977), p.525.
- 14) G. KUSINSKI, D. POLLACK and G. THOMAS, US Patent 6,746,548 (2004).
- 15) G.J. KUSINSKI, D. POLLACK and G. THOMAS, US Patent 6,827,797 (2004).
- 16) J.Y. KOO, M.J. YOUNG and G. THOMAS, Met. Trans. A Vol. 11A, (1980), p.852.
- 17) M. SARIKAYA, A.K. JHINGAN and G. THOMAS, Metallurgical Transactions A 14A, (1983), p.1121.
- 18) D. TREJO, P.J.M. MONTEIRO, J. GERWICK, BEN C. and G. THOMAS, ACI Materials Journal 97, (2000), p.78.
- 19) G.J. KUSINSKI, S.S. FAZA, D. MILLER and G. THOMAS, Proc. 3rd International Engineering and Construction Conference, (2004), ASCE, CD_ROM.
- 20) S.J. BARNARD, G.D.W. SMITH, M. SARIKAYA and G. THOMAS, Scripta Metallurgica 15, (1981), p.387.
- 21) M.X. ZHANG and P.M. KELLY, Materials Characterization 40, (1998), p.159.
- 22) G.H. KOCH, M.P.H. BRONGERS, N.G. THOMPSON, Y.P. VIRMANI and J.H. PAYER, Federal Highway Administration, Washington, D.C., (2001).
- 23) T. NGUYEN and J.W. MARTIN, in "Durability of Building Materials and Components 7", edited by C. Sjoström (E&FN Spon, London, 1996) p. 491.
- 24) W.A. PYC, R.E. WEYERS, D.W. MOKAREM, J. ZEMAJTIS, M.M. SPRINKEL and J.G. DILLARD, Virginia Transportation Research Council, (2000).
- 25) A.A. SAGUES, J.B. LEE, X. CHANG, H. PICKERING, E. NYSTROM, W. CARPENTER, S.C. KRANC, T. SIMMONS, B. BOUCHER and S. HIERHOLZER, Florida D.O.T., (1994).
- 26) G. THOMAS, US Patent 6,273,968 B1 (2001).
- 27) SSINA, in "Designer Handbook", Specialty Steel Industry of North America, (1998).
- 28) G.G. CLEMENÁ, Virginia Transportation Research Council, (2003).